



# An attempt to explain recent trends in European snowfall extremes

Davide Faranda<sup>1,2</sup>

<sup>1</sup>Laboratoire des Sciences du Climat et de l'Environnement, UMR 8212 CEA-CNRS-UVSQ, Université Paris-Saclay, IPSL, 91191 Gif-sur-Yvette, France

<sup>2</sup>London Mathematical Laboratory, 8 Margravine Gardens London, W6 8RH, UK

**Correspondence:** Davide Faranda (davide.faranda@lsce.ipsl.fr)

**Abstract.** The goal of this work is to investigate and explain recent trends in total yearly snow-depth and maximum yearly snow-depth from daily data in light of both the current global warming and the low-frequency variability of the atmospheric circulation. We focus on the period 1979-2018 and compare two different data-sets: the ERA5 reanalysis data and the E-OBSv19 S precipitation data, where snow-depth is identified from rainfall by applying a threshold on temperature. On one hand, we show that the decline in average snow-depth observed in almost all European regions is coherent with the mean global warming and previous findings. On the other hand, we observe contrasting trends in maxima. We argue that this apparent discrepancy between trends in average and maximum snow-depth comes from the subtle effects of atmospheric circulation in driving extreme events and the non-trivial relation with global warming: a warmer Mediterranean Sea may enhance convective precipitation in winter-time and trigger heavy snowfalls. We discuss the limitations of block-maxima indicators and of static identification of trends based on regional or grid-points analysis, paving the way for attributing changes in extreme snowfalls via analogs-based methods.

## 1 Introduction

Heavy snowfalls can have a great impact on economy and society. In January 2017, a cold spell affected most of Eastern and Central Europe and part of southern Europe, causing the death of at least 60 people: The combination of snowfalls with a series of earthquake in Central Italy caused a disastrous avalanche that hit the town of Rigopiano in Abruzzo where a landslide swept and destroyed a hotel, causing several casualties (Frigo et al., 2018). On January 8th, accumulations of 22-23 cm have been measured in some points on the beach of Porto Cesareo, in Apulia. Inland, snow reached and exceeded 2 meters in height on the Apennines. Two further recent examples of snowfalls affecting large populated areas are the February/March 2012 snowstorm in northern Italy with up to 50 cm of snow-depth measured in Bologna (Bisci et al., 2012), and the winter 2018 snowstorm Emma, which affected UK with up to 40cm snow-depth in Wales and the disruption of air and rail transportation in London, Manchester and Liverpool areas (Tonks, 2018).



Besides their cost in terms of societal and economical impacts, these extreme events are often invoked by climate change  
25 denial groups to mystify the public opinion on climate change (Revkin, 2008) and it is therefore important to understand why,  
in an undeniable context of climate change, we do not observe a sharp decrease of their frequency/intensity. Indeed, although  
global temperature rise has driven an overall decrease of average snowfall in past decades (Déry and Brown, 2007) and this  
decreasing trend is expected to continue in future “business-as-usual” emission scenarios (Brutel-Vuilmet et al., 2013), it is not  
clear whether the same conclusions hold for extreme snowstorm events. Atmospheric extreme weather events do not always  
30 have a trivial relation with average global warming (Murray and Ebi, 2012). The goal of this paper is to shed a light on recent  
trends in extreme snowfalls, by projecting the recent changes in frequency/intensity of extreme snowfalls on the large scale  
(synoptic) dynamical drivers and identifying possible small scale convective thermodynamic feedback.

Heavy snowfalls over large populated areas are often associated to synoptic atmospheric phenomena, namely extratropical  
35 cyclones traveling southwards in jet-stream meanders (Tibaldi and Buzzi, 1983; Barnes et al., 2014; Lehmann and Coumou,  
2015) associated to the disruption of the westerly flow. Mid-latitude atmospheric dynamics is driven by oscillations of the jet  
stream (Wallace and Hobbs, 2006). Its strongest winds correspond to maxima of temperature gradients. Cold air is normally  
confined north stream and it is mixed to subtropical warm air only through the destabilization of the jet, with a disruption of  
the normal westerly flow by disturbances usually triggered by anticyclone wave breaking (Lehmann and Coumou, 2015). This  
40 effect propagates upward in the stratosphere and can weaken or even reverse the westerly flow in the stratospheric jet-stream,  
leading to a compression of stratospheric air, measurable with a rapid warming, up to 50°C in few days (McIntyre and Palmer,  
1983). It then propagates back to the troposphere, forcing the jet stream further south and leading to the development of block-  
ing high pressure systems at higher latitudes (Wang and Chen, 2010). Blocking conditions create a dipole consisting of high  
pressure structures over some regions and low pressure systems (extratropical cyclones) travelling southward in other regions.  
45 If these blocking highs become established close to Greenland, cold air from polar latitudes can be advected towards western  
Europe, causing extreme snowfalls over UK, France, Benelux and the Iberian Peninsula. If the high pressure ridge is positioned  
in the Icelandic region, cold air coming from Russia or Scandinavia flows in the Mediterranean Sea and leads to extreme snow-  
falls over Italy, the Balkans, Greece and Turkey (Buehler et al., 2011). Since the modifications of the jet-stream dynamics are  
fundamental drivers of extreme snowfalls, understanding the response of atmospheric circulation to anthropogenic forcing is  
50 the first step to track the modifications in extreme snowfalls frequency/intensity and assess whether the changes in frequency  
and intensity are due to long term variability of the atmospheric circulation or induced by anthropogenic forcing (Strong et al.,  
2009; Overland and Wang, 2010; Wu and Zhang, 2010; Deser et al., 2017). It is particularly important to determine whether  
the mid-latitude flows favour zonal or meridional patterns with changing anthropogenic forcing. It has been so far very diffi-  
cult to prove any significant shift in the dynamical patterns observed at mid-latitudes (Shepherd, 2014). Existing studies are  
55 not conclusive enough to determine whether large scale drivers will modify frequency/intensity of extreme snowfalls under  
anthropogenic forcing. On one side, Cohen et al. (2014) and Kim et al. (2014) showed that the recent increase of temperatures  
in the Arctic is associated to an amplification of planetary waves, affecting storm tracks and leading to enhanced winter con-  
ditions. On the other hand, several authors found a zonalization of the mid-latitude flow (Lorenz and DeWeaver, 2007; Chen



et al., 2016; Screen et al., 2014; Faranda et al., 2019) and a minimal or even undetectable effect of the Arctic sea-ice on the  
60 meandering of the jet at mid-latitudes (Blackport et al., 2019; Screen, 2017; Screen et al., 2018).

Although heavy snowfalls are driven by the large scale atmospheric circulation, their effects can be greatly enhanced by  
local geographic constraints and thermodynamic feedbacks Lüthi et al. (2019). Local features like the Alps in Europe or the  
Great Lakes in USA may increase precipitation and provide relevant feedback to extreme snowfalls (Niziol et al., 1995). A  
65 similar mechanisms exist also for the Mediterranean sea, as recently detailed in D’Errico et al. (2019). The mid-tropospheric  
cold winter air advection associated with the synoptic patterns flows over the relatively warmer waters of the Mediterranean  
sea and picks up water vapor from the lake surface. This warmer and wetter air rises and cools as it moves away from the  
sea towards land areas forming convective clouds that transform moisture into snow. In the mountainous topography of the  
European continent, this phenomenon can be extremely powerful in triggering heavy snowfalls (D’Errico et al., 2019). We will  
70 also consider this effect in driving convection via the analysis of precipitation patterns during extreme events.

The remaining of the paper is organized as follows. In section 2, we describe the data-sets used in this study and the  
difficulties arising in assessing the quality of snow data. In section 3 we compute the trends and discuss the consistence of the  
trends among the data-sets. In section 4 we explain the largest trends in heavy snowfalls in light of the atmospheric circulation.  
75 Conclusions are presented in section 5.

## 2 Data and Methods

Good quality snow data at synoptic or regional scales are difficult to obtain (Rasmussen et al., 2012). From an observational  
point of view, quality observational data-sets exist only at high mountains sites and in regions where snowfalls are recurrent  
phenomena. Excellent snow data-sets exist for Scandinavian countries as well as for the Alpine regions (Auer et al., 2005;  
80 Scherrer and Appenzeller, 2006; Isotta et al., 2014). Our goal is however to study trends at a European level and to focus on  
regions where snowfalls are rare. We have therefore to rely on reanalyses as well as on gridded observational data. In this study  
we analyse the period 1979-2018 and use a reanalysis product (ERA5) as well as gridded observations data-set (E-OBSv19.0).  
The reference data-set will be ERA5 (C3S), a very recent product by the ECMWF with high resolution ( $0.25^\circ$  horizontal res-  
olution) and accurate physical parametrizations. For the observations, we use E-OBSv19 ( $0.25^\circ$  horizontal resolution) which  
85 contains gridded temperatures and precipitations observations (Cornes et al., 2018).

Another problem in comparing snow data issued from different sources is the choice of the variable associated to snow-  
falls (Nitu and Wong, 2010). Snowfall can both be measured from precipitation (snow water equivalent), or from accumulation  
on the ground (snow-depth). Both the measurements have pros and cons. Snow water equivalent (SWE) is obtained by melting  
90 snow falling inside a heated rain gauge and it is expressed in  $\text{Kg/m}^2$  or mm. An advantage of using this variable is the accuracy  
of the measurement. For obvious reasons, SWE is mostly used by hydrologists as it has a direct connection with runoff and



rivers discharge. Since the snow is immediately transformed into water, SWE does not distinguish between snowfalls which produced accumulations on the ground or not. The other quantity, namely the snow-depth (SD), is a measure of the snow height on the ground and it can be affected by several problems due to gravitational settling, wind packing, melting and re-crystallization. SD is a quantity of interest for its societal impact: large SD amounts correspond the snow to be removed to free ground transportation infrastructures. In this paper we will therefore use daily SD and express it in cm. We now explain how to get this quantity from the different data-sets considered in this study.

- For ERA5 [80W-50E,22.5N-70N], we use the accumulated total snow that has fallen to the Earth's surface. From the ECMWF description, this quantity consists of both snow due to the large-scale atmospheric flow and convective precipitations. It measures the total amount of water accumulated from the beginning of the forecast time to the end of the forecast step. This quantity is higher than the snow-depth if snow has melted during the period over which this variable was accumulated. The units given measure the depth the water would have if the snow melted and was spread evenly over the grid box. We get the snowfall from hourly data and construct the daily SD by summing up the snowfall in intervals of 24 hours. We chose ERA5 data-set as the preferential one for our study because of its physical consistency and the use of advance assimilation techniques for its compilation. Besides the nominal  $0.25^\circ$  horizontal resolution, we will also compute the statistic over the NUTS-2 regions, this scale being the one used by European stakeholders to assess impacts.
- For E-OBSv19.0 [40.375W-50E,25.375N-75.375N] only lands points, we do not dispose directly of snowfall, SWE or SD data. We have to infer them from daily total precipitation and daily mean temperature data. We apply a simple algorithm which consists of considering as snowfall all precipitations occurred in days where the average temperature is below  $2^\circ$  C. Of course with this method we can have false positive as well as false negative events, but we have verified (not shown) that results on the trends do not depend qualitatively from the threshold providing that it is chosen between  $0^\circ$  C and  $2.5^\circ$  C. Since we use a threshold of  $2^\circ$  C, some of the precipitation would not be snowfall. In order to avoid overestimation we consider SD only  $2/3$  of the daily amount obtained.

We now present the climatology for the two data-sets used in this study and focus on two quantities: yearly total snow-depth SD (average 1979-2018 in Figure 1a,c,e) and the maximum yearly (block maxima) snow-depth SD from daily data (average 1979-2018 in Figure 1b,d,f) for the three data-sets. Despite local differences, we can remark a substantial agreement among all data-sets for the two variables considered. We remind that E-OBSv19 data are defined only for land points. The agreement between the ERA5 and the E-OBSv19.0 data-set is remarkable, with the latter showing generally lower SD, possibly due to our choice of the factor  $2/3$  when converting precipitation into snow. Analysing the climatology we remark that, at southern latitudes and on the plains, mean and max statistics tend coincide because the number of snow days per year is limited, i.e. all snowfall is concentrated in one or few events.



### 3 Trends computations

Linear trends (hereinafter just trends) are computed per decades on both the yearly total SD and the maximum yearly SD. Results are shown in Figure 2 for ERA5 (a,b) and E-OBSv19.0 (b,d). Figure 3 shows the p-values of the trends multiplied by the sign of the trends. For the yearly total SD (a,c) trends are negative in ERA5 for most of Northern, Central and Eastern Europe (a), whereas for E-OBSv19.0 some positive trends are observed on Eastern Europe, Scandinavian mountain ranges and Greece. Overall there is agreement between the two data-sets in Central and Western Europe. The difference in the trends between ERA5 and E-OBSv19.0 could be due to the over-estimation of snow precipitation due to the temperature threshold imposed. For the maximum yearly SD, trends observed are generally milder and very scattered. There is however a certain agreement in the positive trends over eastern Europe and negative trends over western Europe (excluding Spain) among the two data-sets.

When looking at the significance of the trends (Figure 3) the picture is rather coherent: for both the data-sets, only negative trends over Western and northern Europe are significant. This is compatible with the findings of Déry and Brown (2007) showing that the warming of the northern Atlantic observed in the last decades have contributed to a decrease of snowfalls in this region. Significance of trends is however more sparse for the maxima in both data-sets. We do observe fewer negative and some positive significant trends over the domain considered. This suggests a non-trivial relation between the occurrence of extreme snowfalls, global mean warming and the internal, long-term variability of the atmospheric circulation.

### 4 Large scale atmospheric dynamics associated to extreme snowfalls

In order to understand the origins of the trends, we should analyse the events leading to maximum snowfalls at each grid point from both a dynamical and thermodynamic point of view. From Figures 2-3 we have seen that trends are very scattered and even adjacent grid points can show trends of different signs. This makes the single grid-point analysis almost meaningless as robust links between SD and large scale fields cannot be identified. We move therefore from the single grid-point description to an aggregate analysis obtained by averaging the ERA5 data per NUTS2 region. The average is performed on the hourly data. The same statistics presented in Figures 1-3 are displayed in Figure 4 for the NUTS2 regions. Figure 4-a,b) show that the climatology of total yearly SD and maximum SD is preserved when aggregating data. Moreover, coarse-graining the data on NUTS2 regions also provides a more coherent picture of the trends (Figure 4-c,d). Indeed for yearly total SD, all regions but Spain and southern Italy show negative significant (Figure 4e) trends. For maximum yearly SD, trends are negative in central Europe and positive on the Mediterranean regions. Significance for trends in maximum yearly SD (Figure 4-f) is more sparse but we have several regions with both negative and positive significant trends.

150

From now on we stick to the analysis of the ERA5-NUTS2 data. We decide to use ERA5 because snowfalls are produced by the model underlying the reanalysis and naturally associated to coherent circulation patterns. We discard the E-OBSv19.0 dataset as it does not contain other variables that could help in tracking the atmospheric circulation, such as the sea-level pressure or the geopotential height. Sticking to ERA5, we identify the 10 regions having the largest positive and negative trends. In this



155 section we focus on the intensity of positive or negative trends regardless of their significance. As pointed out by (Altman and  
Krzywinski, 2017), statistical testing based on p-values presents several limitations, and can produce misleading results even  
in designed experiments. Here, we privilege the physical complexity of the phenomenon, as information about pure statistical  
significance has already been discussed in the previous section. In Figure 5 we show the box-plots of the yearly maxima or-  
ganized in two different periods (1979-1998 and 1999-2018) for the 10 regions having the largest positive (a) and negative (b)  
160 trends in maxima of SD. The insets of Figure 5 show the location of the regions with largest trends and the magnitude of the  
trends (size of disks). Largest positive trends are located mostly in the Balkans. It is interesting to observe how boxplots and  
trends provide a different information: for ITF1 (Abruzzo region, in Italy) we detect the largest positive trend, but the bulk of  
the distribution (visualized by the colored bar in the boxplot) shifts instead to lower values. The increasing trend is therefore  
largely due to the two outliers. Another example is TR42 (Kocaeli, Turkey), where we have a small trends but a large positive  
165 shift in the distribution.

We now analyse the relation between largest trends and the long-term changes of the atmospheric patterns associated to  
these events. We divide the sample into two periods: 1979-1998 and 1999-2018 and consider three different atmospheric fields:  
the daily averaged geopotential height at 500 hPa (Z500) as a tracer of the atmospheric circulation (Jézéquel et al., 2018), the  
170 daily averaged two-meters temperature (T2M) to account for thermodynamic changes and the snow-depth (SD). We prefer  
the Z500 variable to the sea-level pressure because the latter shows a strong variability during these events: when computing  
median and mean sea-level pressure fields associated to these events we observe that they do not produce similar patterns. For  
each region and each period, we average the fields corresponding to the days when the yearly maxima of SD are observed. We  
then subtract the average for the first period from that of the second one obtaining the anomaly fields displayed in Figure 6  
175 (Z500), Figure 7 (T2M) and Figure 8 (SD). We report the results only for the 10 regions displaying the largest negative  
(panels in the red frame) and positive trends (panels in the blue frame). For Z500 (Figure 6) we remark positive anomalies  
for regions showing largest negative trends. This implies that circulation patterns associated to recent heavy snowfalls display  
higher geopotential heights (weaker cyclonic structure) than maximum SD events in the 1979-1998 period. It is interesting  
to note how the anomalies show preferentially an anti-zonal or a blocked pattern, with negative Z500 anomalies generally  
180 concentrated over eastern Europe. As one would expect in a warming climate, the T2M anomalies (Figure 7-red panels) are  
generally positive, except for CZ03 (Jihozápad, Czech Republic). The analysis of SD for CZ03 (Figure 8) indicates that the  
area corresponding to positive anomalies is quite limited and that the surrounding regions receive more snowfalls during these  
events, hinting to a rather localized effect. Similarly, Gaziantep Subregion (TRC1) shows positive SD anomalies but most of  
western Turkey have anomalies of opposite sign.

185 For the largest positive trends, we can divide regions into groups with similar characteristics. ITF1 region (Abruzzo, in Italy)  
has the largest positive trend and it can be grouped with BA36, BA34 and BA21 (Bosnia and Herzegovina) and ME00 (Mace-  
donia) regions: from Figure 8 we can observe that negative SD anomalies in ITF1 correspond to negative anomalies in the  
Bosnia and Herzegovina regions and viceversa. There is no clear geopotential anomaly (Figure 6), nor evident T2M anomalies  
(Figure 7) associated to those events. To explain the trends, we can use the results obtained by D'Errico et al. (2019) in an





190 event-based study of cold and snowy spells over Italy. There, the positive trends in snowfalls on the Adriatic regions were linked to the enhancement of convective precipitations from the Mediterranean sea, which is warming faster than the oceans at same latitudes because of its closed geometry (Gualdi et al., 2013). Convective precipitations can be observed even without a real cyclogenesis on the Adriatic sea, just as an effect of the intrusion of very cold air from the Balkans. For CH5 (Eastern Switzerland), the pattern of Z500 anomaly, showing deeper geopotential heights over the Iberian peninsula, tends to suggest  
195 a stronger meridional flux. This pattern can favour large snowfalls on the alpine ridge, thus explaining the positive trend. For Turkish regions (TR41, TR33 and TR42), a negative geopotential anomaly (Figure 6) is indeed associated to deeper cyclones leading to more intense snowfalls in the 1999-2018 years. The T2M (Figure 7) and SD anomalies (Figure 8) are negative over a large portion of the Anatolian peninsula, supporting this picture.

200 The last analysis aims at identifying possible seasonal variations of extreme snowfalls. Figure 9 shows individual SD maxima (small dots), averages (big dots) and average time of the year of maxima occurrence (stars) for the two different periods (1999-2018 magenta, 1979-1998 black). The angle corresponds to a date of the year in counterclockwise sense. The radius show SD magnitude relative to the largest recorded value. For the regions showing the largest negative trends (red frame) change in seasonality of maxima occurrence do not show an evident, common shift. Results are more interesting for regions showing  
205 largest positive trends (blue frame) where for 8/10 regions there is a shift towards anticipating the maxima. A supporting physical argument for these shifts could be the warming trend in the Mediterranean sea enhancing, early in the winter season, convective snow precipitations through the availability of humidity and potential energy (D'Errico et al., 2019).

## 5 Conclusions

We have analysed recent trends in yearly total and maximum snow-depth SD from ERA5 reanalysis and the E-OBSv19.0 data-  
210 sets. Even though the two products show large differences in trends, we have identified a robust signal in the general decrease in the yearly total snow-depth, in particular for Northern and Western Europe. For SD maxima, trends are more contrasted: negative trends persist over Western Europe, but over the Mediterranean area we identified a certain number of regions showing positive trends.

This discrepancy between average and extreme SD trends is compatible with future scenarios for winter Mediterranean pre-  
215 cipitations. Polade et al. (2017) project an overall decrease of winter average precipitations over the Mediterranean sea, but an increase of extreme precipitations and of their variability. Extremes should be favored by a warmer sea, with a larger variability of moisture and potential energy. They could also benefit from blocking patterns forcing southward movement of polar extratropical cyclones towards Europe (Liu et al., 2012). Our analysis of the atmospheric circulation associated to maxima snowfalls suggests that these blocking patterns are crucial in determining heavy snowfalls (Figure 6). From the analysis of 500  
220 hPa geopotential height patterns in the last 20 years, we observe more anticyclonic conditions over Western Europe associated to cyclonic conditions over Eastern Europe. This explains both the negative trends over western Europe and the positive trends over the Balkans regions and Turkey. Even though this could suggest a relation between our finding and the arctic amplifi-



cation caused by climate change (Vavrus et al., 2017), we stress that the length of the data-sets used is too short to attribute these trends to climate change and that they could be produced by the inter-decadal variability of the atmospheric circulation.  
225 Recent studies on whether these patterns are due to low-frequency variability of the Atlantic circulation or to climate change are debated (see, e.g., the discussion in Screen (2017)).

This study comes with some caveats. First of all, the trends (especially those on the maxima) depend on the datasets chosen. Here we have trusted ERA5 because of the high resolution and the consistent representation of snowfalls with the atmospheric circulation. The lack of longer and highly resolved data-sets for snowfall is a strong limitation and it adds up to the intrinsic dif-  
230 ficulty of simulating snowfalls process due to their highly non-linear behavior and the fact they involve phase transitions. Our study also highlights the limitation in the use of a static approach based on the block-maxima procedure for the computation of trends. As seen for some of the regions showing the largest trends, extreme events are spatially extended over different regions and they are caused by precise dynamical patterns. These limitations can be overcome by a pattern-based approach, where heavy snowfalls are identified by analogs techniques using maps of atmospheric variables (Yiou et al., 2013), and following  
235 their evolution in time.

## 6 Acknowledgments

The author wishes to thank F Pons, S Fromang, P Yiou, M Vrac for the discussions and S Thao for the help with the ERA5 dataset. The author acknowledges the support of the INSU-CNRS-LEFE-MANU grant (project DINCLIC), as well as EUPHEME and DAMA.

240 *Competing interests.* The author declares no competing interest.





## References

- Altman, N. and Krzywinski, M.: Points of significance: interpreting P values, 2017.
- Auer, I., Böhm, R., Jurković, A., Orlik, A., Potzmann, R., Schöner, W., Ungersböck, M., Brunetti, M., Nanni, T., Maugeri, M., et al.: A new instrumental precipitation dataset for the greater alpine region for the period 1800–2002, *International Journal of Climatology: A Journal of the Royal Meteorological Society*, 25, 139–166, 2005.
- 245 Barnes, E. A., Dunn-Sigouin, E., Masato, G., and Woollings, T.: Exploring recent trends in Northern Hemisphere blocking, *Geophysical Research Letters*, 41, 638–644, 2014.
- Bisci, C., Fazzini, M., Beltrando, G., Cardillo, A., and Romeo, V.: The February 2012 exceptional snowfall along the Adriatic side of Central Italy, *Meteorologische Zeitschrift*, 21, 503–508, 2012.
- 250 Blackport, R., Screen, J. A., van der Wiel, K., and Bintanja, R.: Minimal influence of reduced Arctic sea ice on coincident cold winters in mid-latitudes, *Nature Climate Change*, 9, 697–704, 2019.
- Brutel-Vuilmet, C., Menegoz, M., and Krinner, G.: An analysis of present and future seasonal northern hemisphere land snow cover simulated by CMIP5 coupled climate models., *Cryosphere*, 7, 2013.
- Buehler, T., Raible, C. C., and Stocker, T. F.: The relationship of winter season North Atlantic blocking frequencies to extreme cold or dry spells in the ERA-40, *Tellus A: Dynamic Meteorology and Oceanography*, 63, 174–187, 2011.
- 255 (C3S), C. C. C. S.: ERA5: Fifth generation of ECMWF atmospheric reanalyses of the global climate, 2017.
- Chen, H. W., Zhang, F., and Alley, R. B.: The robustness of midlatitude weather pattern changes due to Arctic sea ice loss, *Journal of Climate*, 29, 7831–7849, 2016.
- Cohen, J., Screen, J. A., Furtado, J. C., Barlow, M., Whittleston, D., Coumou, D., Francis, J., Dethloff, K., Entekhabi, D., Overland, J., et al.: 260 Recent Arctic amplification and extreme mid-latitude weather, *Nature geoscience*, 7, 627–637, 2014.
- Cornes, R. C., van der Schrier, G., van den Besselaar, E. J., and Jones, P. D.: An Ensemble Version of the E-OBS Temperature and Precipitation Data Sets, *Journal of Geophysical Research: Atmospheres*, 123, 9391–9409, 2018.
- D’Errico, M., Yiou, P., Nardini, C., Lunkeit, F., and Faranda, D.: Warmer Mediterranean temperatures do not decrease snowy cold spell intensity over Italy, *Scientific Reports (under review)*, 2019.
- 265 Déry, S. J. and Brown, R. D.: Recent Northern Hemisphere snow cover extent trends and implications for the snow-albedo feedback, *Geophysical Research Letters*, 34, 2007.
- Deser, C., Hurrell, J. W., and Phillips, A. S.: The role of the North Atlantic Oscillation in European climate projections, *Climate dynamics*, 49, 3141–3157, 2017.
- Faranda, D., Alvarez-Castro, M. C., Messori, G., Rodrigues, D., and Yiou, P.: The hammam effect or how a warm ocean enhances large scale atmospheric predictability, *Nature communications*, 10, 1316, 2019.
- 270 Frigo, B., Chiaia, B., Chiambretti, I., Bartelt, P., Maggioni, M., and Freppaz, M.: The January 18th 2017 Rigopiano disaster in Italy—analysis of the avalanche dynamics, in: *Proc. Intl. Snow Science Workshop, Innsbruck, Austria*, pp. 6–10, 2018.
- Gualdi, S., Somot, S., Li, L., Artale, V., Adani, M., Bellucci, A., Braun, A., Calmanti, S., Carillo, A., Dell’Aquila, A., et al.: The CIRCE simulations: regional climate change projections with realistic representation of the Mediterranean Sea, *Bulletin of the American Meteorological Society*, 94, 65–81, 2013.
- 275



- Isotta, F. A., Frei, C., Weilguni, V., Perčec Tadić, M., Lassegues, P., Rudolf, B., Pavan, V., Cacciamani, C., Antolini, G., Ratto, S. M., et al.: The climate of daily precipitation in the Alps: development and analysis of a high-resolution grid dataset from pan-Alpine rain-gauge data, *International Journal of Climatology*, 34, 1657–1675, 2014.
- Jézéquel, A., Yiou, P., and Radanovics, S.: Role of circulation in European heatwaves using flow analogues, *Climate dynamics*, 50, 1145–1159, 2018.
- Kim, B.-M., Son, S.-W., Min, S.-K., Jeong, J.-H., Kim, S.-J., Zhang, X., Shim, T., and Yoon, J.-H.: Weakening of the stratospheric polar vortex by Arctic sea-ice loss, *Nature communications*, 5, 4646, 2014.
- Lehmann, J. and Coumou, D.: The influence of mid-latitude storm tracks on hot, cold, dry and wet extremes, *Scientific reports*, 5, 17 491, 2015.
- Liu, J., Curry, J. A., Wang, H., Song, M., and Horton, R. M.: Impact of declining Arctic sea ice on winter snowfall, *Proceedings of the National Academy of Sciences*, 109, 4074–4079, 2012.
- Lorenz, D. J. and DeWeaver, E. T.: Tropopause height and zonal wind response to global warming in the IPCC scenario integrations, *Journal of Geophysical Research: Atmospheres*, 112, 2007.
- Lüthi, S., Ban, N., Kotlarski, S., Steger, C. R., Jonas, T., and Schär, C.: Projections of Alpine Snow-Cover in a High-Resolution Climate Simulation, *Atmosphere*, 10, 463, 2019.
- McIntyre, M. E. and Palmer, T.: Breaking planetary waves in the stratosphere, *Nature*, 305, 593, 1983.
- Murray, V. and Ebi, K. L.: IPCC special report on managing the risks of extreme events and disasters to advance climate change adaptation (SREX), 2012.
- Nitu, R. and Wong, K.: CIMO survey on national summaries of methods and instruments for solid precipitation measurement at automatic weather stations, WMO, 2010.
- Niziol, T. A., Snyder, W. R., and Waldstreicher, J. S.: Winter weather forecasting throughout the eastern United States. Part IV: Lake effect snow, *Weather and Forecasting*, 10, 61–77, 1995.
- Overland, J. E. and Wang, M.: Large-scale atmospheric circulation changes are associated with the recent loss of Arctic sea ice, *Tellus A*, 62, 1–9, 2010.
- Polade, S. D., Gershunov, A., Cayan, D. R., Dettinger, M. D., and Pierce, D. W.: Precipitation in a warming world: Assessing projected hydro-climate changes in California and other Mediterranean climate regions, *Scientific reports*, 7, 10 783, 2017.
- Rasmussen, R., Baker, B., Kochendorfer, J., Meyers, T., Landolt, S., Fischer, A. P., Black, J., Thériault, J. M., Kucera, P., Gochis, D., et al.: How well are we measuring snow: The NOAA/FAA/NCAR winter precipitation test bed, *Bulletin of the American Meteorological Society*, 93, 811–829, 2012.
- Revkin, A.: Skeptics on human climate impact seize on cold spell, *The New York Times*, 2, 2008.
- Scherrer, S. C. and Appenzeller, C.: Swiss Alpine snow pack variability: major patterns and links to local climate and large-scale flow, *Climate Research*, 32, 187–199, 2006.
- Screen, J. A.: The missing Northern European winter cooling response to Arctic sea ice loss, *Nature communications*, 8, 14 603, 2017.
- Screen, J. A., Deser, C., Simmonds, I., and Tomas, R.: Atmospheric impacts of Arctic sea-ice loss, 1979–2009: Separating forced change from atmospheric internal variability, *Climate dynamics*, 43, 333–344, 2014.
- Screen, J. A., Deser, C., Smith, D. M., Zhang, X., Blackport, R., Kushner, P. J., Oudar, T., McCusker, K. E., and Sun, L.: Consistency and discrepancy in the atmospheric response to Arctic sea-ice loss across climate models, *Nature Geoscience*, 11, 155–163, 2018.
- Shepherd, T. G.: Atmospheric circulation as a source of uncertainty in climate change projections, *Nature Geoscience*, 7, 703–708, 2014.



- Strong, C., Magnúsdóttir, G., and Stern, H.: Observed feedback between winter sea ice and the North Atlantic Oscillation, *Journal of Climate*,  
315 22, 6021–6032, 2009.
- Tibaldi, S. and Buzzi, A.: Effects of orography on Mediterranean lee cyclogenesis and its relationship to European blocking, *Tellus A: Dynamic Meteorology and Oceanography*, 35, 269–286, 1983.
- Tonks, A.: Storm Emma in pictures: Worst snow storm to hit the UK in 50 years, *The Express*, 2018.
- Vavrus, S. J., Wang, F., Martin, J. E., Francis, J. A., Peings, Y., and Cattiaux, J.: Changes in North American atmospheric circulation and  
320 extreme weather: Influence of Arctic amplification and Northern Hemisphere snow cover, *Journal of Climate*, 30, 4317–4333, 2017.
- Wallace, J. M. and Hobbs, P. V.: *Atmospheric science: an introductory survey*, vol. 92, Elsevier, 2006.
- Wang, L. and Chen, W.: Downward Arctic Oscillation signal associated with moderate weak stratospheric polar vortex and the cold December  
2009, *Geophysical Research Letters*, 37, 2010.
- Wu, Q. and Zhang, X.: Observed forcing-feedback processes between Northern Hemisphere atmospheric circulation and Arctic sea ice  
325 coverage, *Journal of Geophysical Research: Atmospheres*, 115, 2010.
- Yiou, P., Salameh, T., Drobinski, P., Menut, L., Vautard, R., and Vrac, M.: Ensemble reconstruction of the atmospheric column from surface  
pressure using analogues, *Climate dynamics*, 41, 1333–1344, 2013.

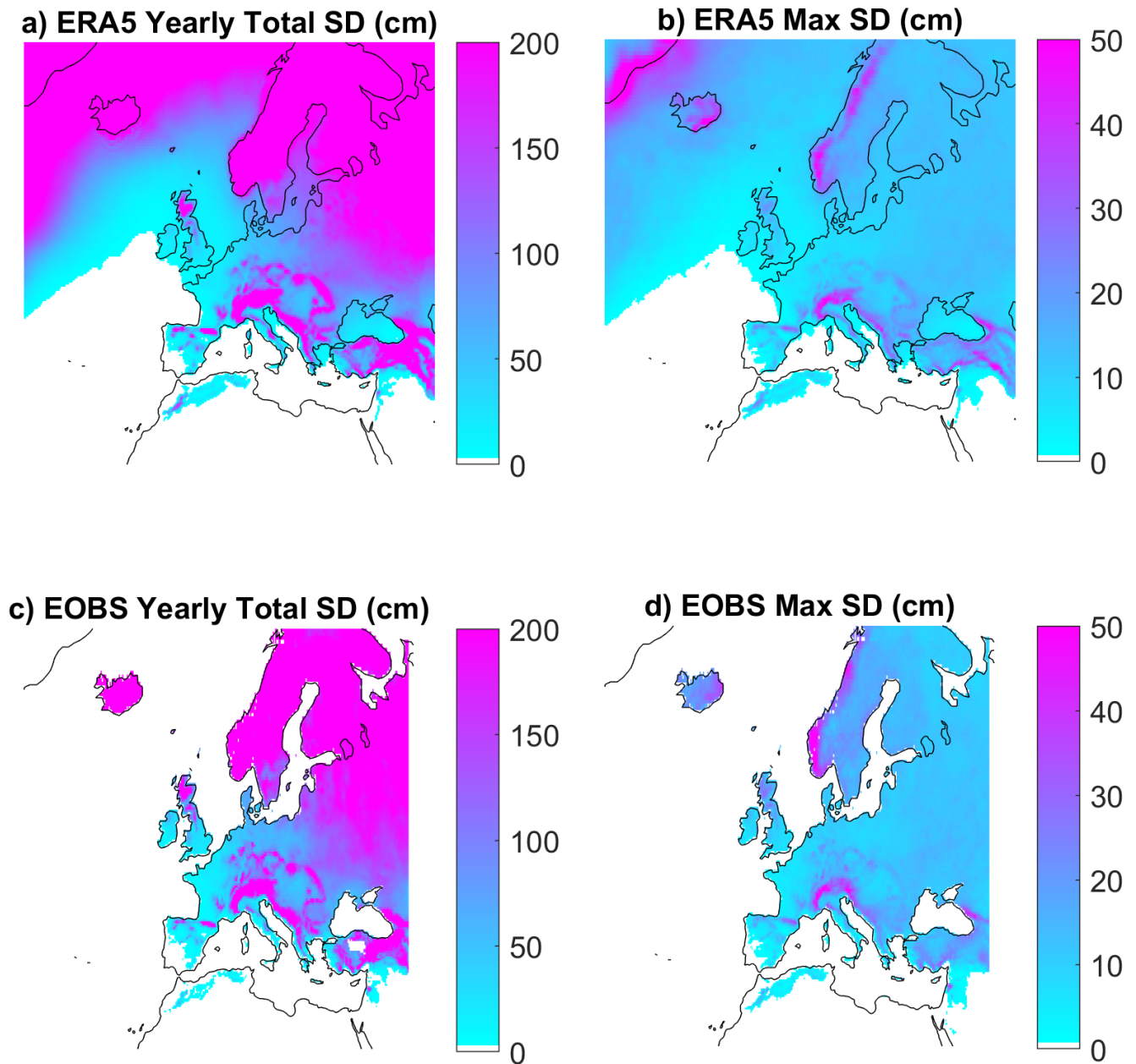


**Figure 1.** a,c) Yearly total snow-depth SD (average 1979-2018) b,d) maximum yearly snow-depth SD from daily data (average 1979-2018) for the ERA5 (a,b), E-OBSv19.0 (c,d) data-sets.

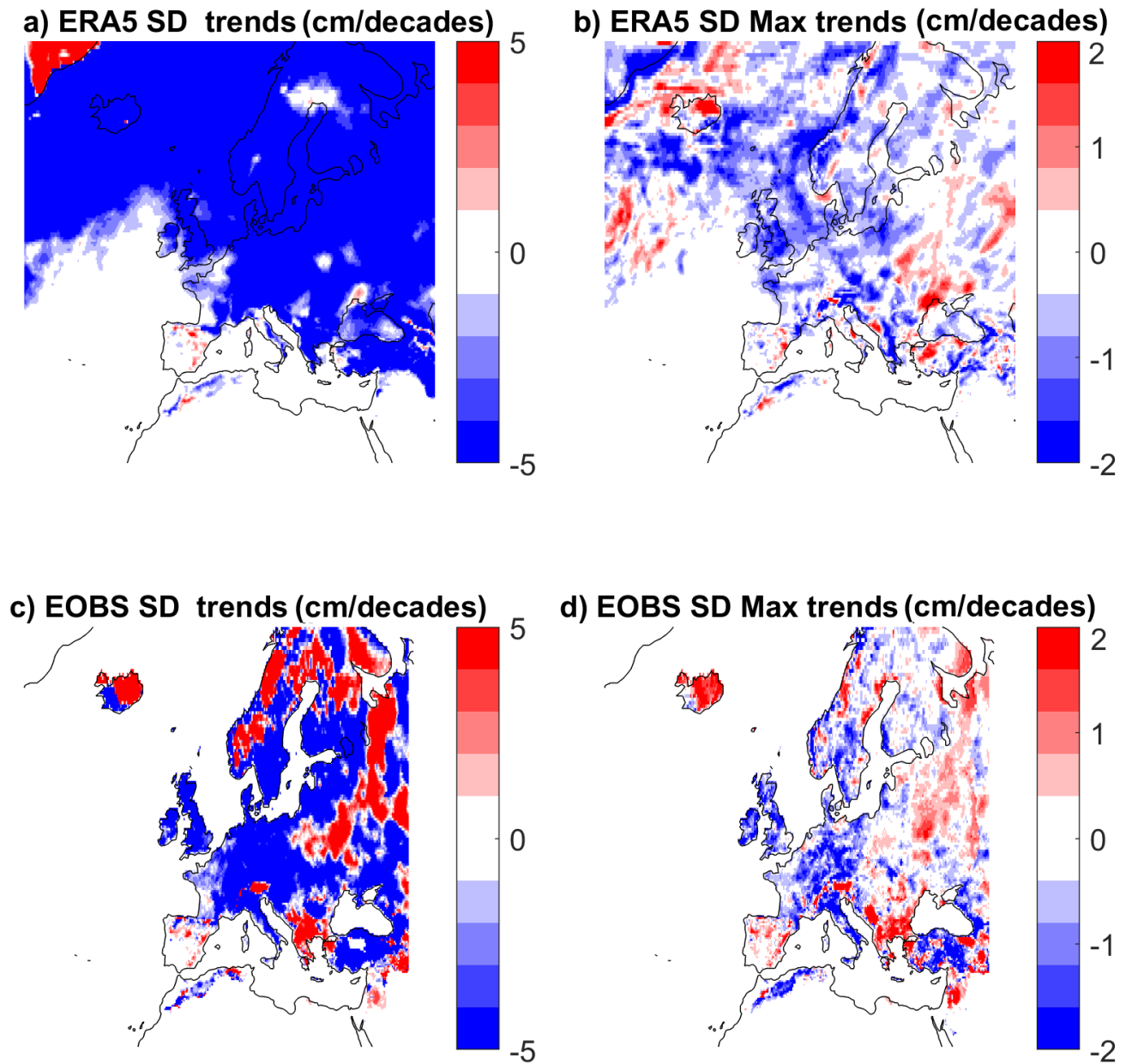
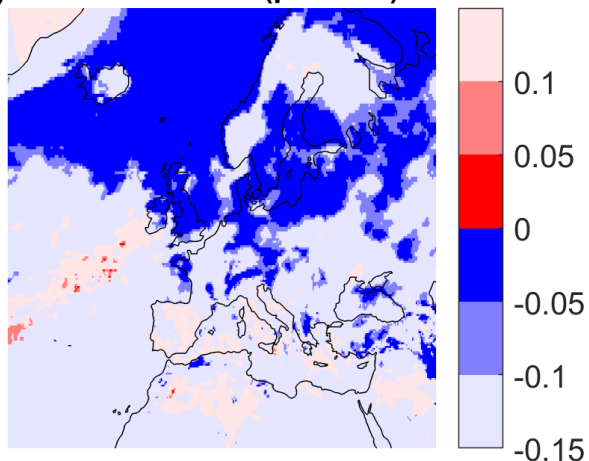


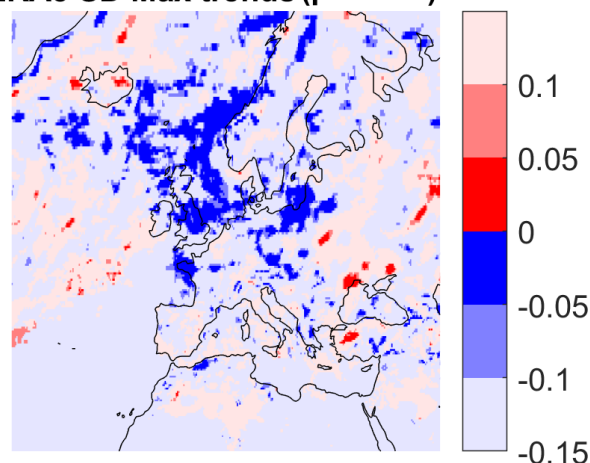
**Figure 2.** a,c) Trends (cm/decades) in yearly total snow-depth SD (1979-2018) b,d) Trends (cm/decades) in maximum yearly snow-depth SD from daily data (1979-2018) for the ERA5 (a,b), E-OBSv19.0 (c,d) data-sets.



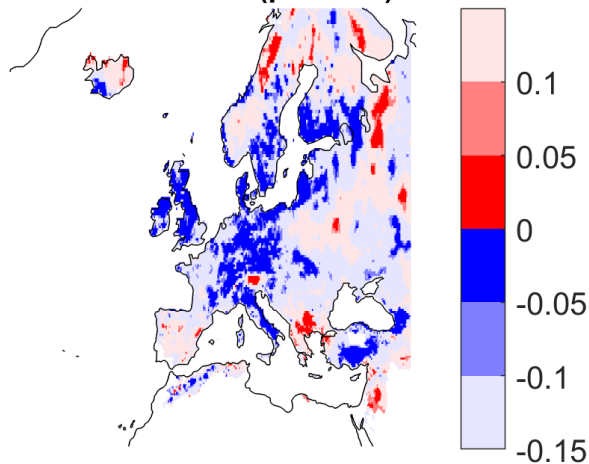
a) ERA5 SD trends (pvalues)



b) ERA5 SD Max trends (pvalues)



c) EOBS SD trends (pvalues)



d) EOBS SD Max trends (pvalues)

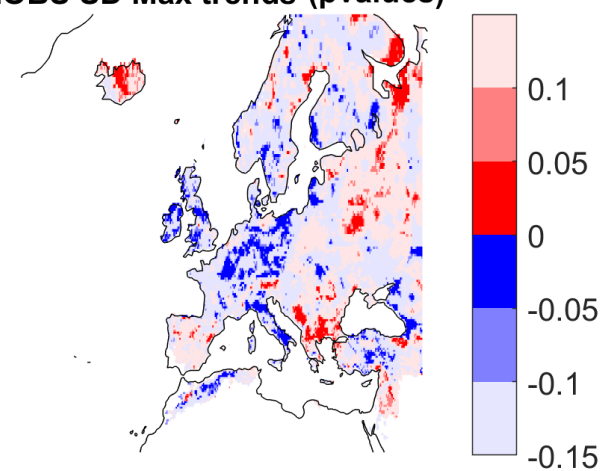


**Figure 3.** a,c) Significant trends (p-values) in yearly total snow-depth SD (1979-2018) b,d) Significant trends (p-values) in maximum yearly snow-depth SD from daily data (1979-2018) for the ERA5 (a,b), E-OBSv19.0 (c,d) data-sets.



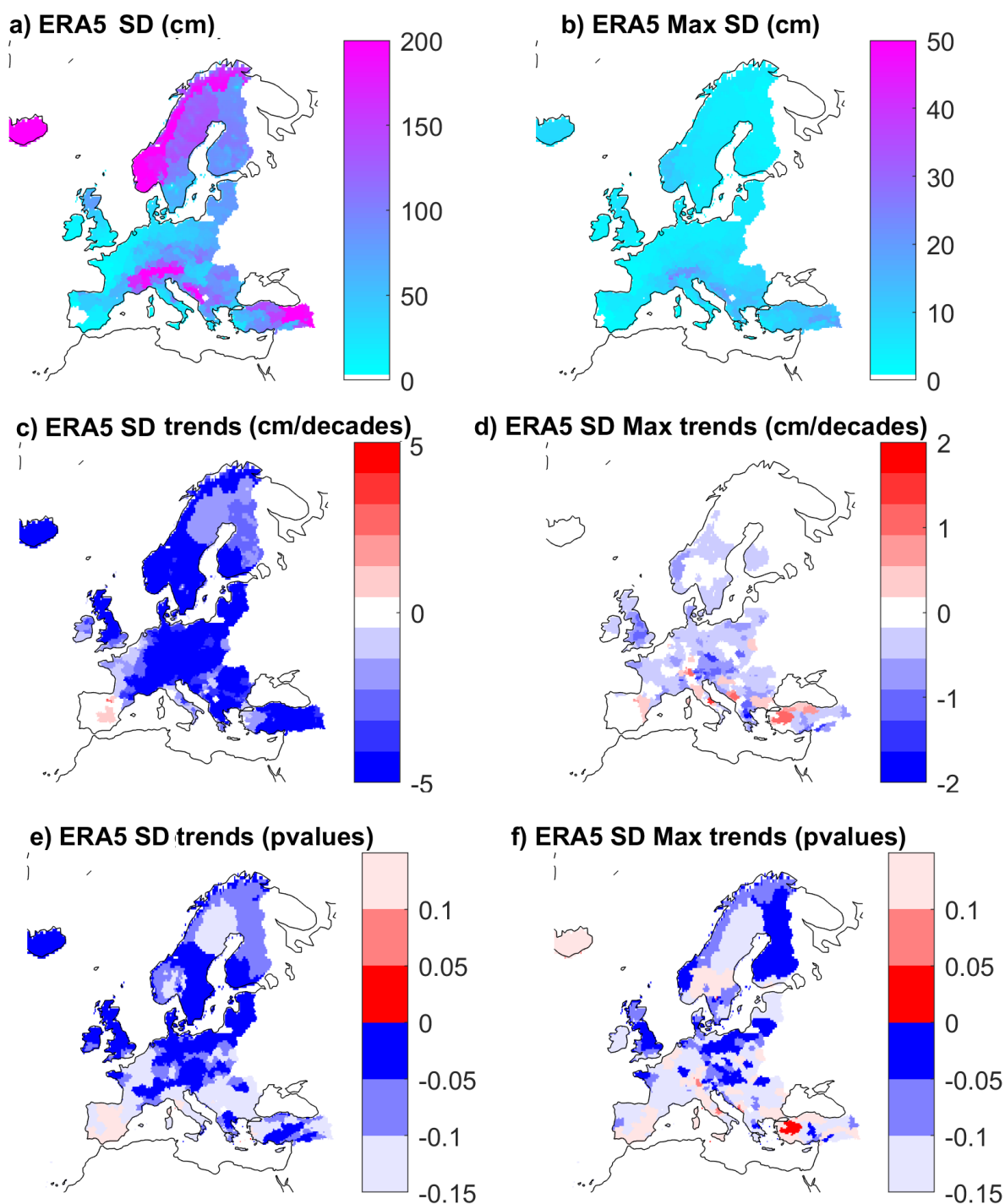


**Figure 4.** a) Yearly total snow-depth SD , b) maximum yearly snow-depth SD from daily data, c) Trends (cm/decades) in yearly total snow-depth SD, d) Trends (cm/decades) in maximum yearly snow-depth SD from daily data, e) significant trends (p-values) in yearly total snow-depth SD, f) Significant trends (p-values) in maximum yearly snow-depth SD from daily data for the ERA5 1979-2018 NUTS2 regions.



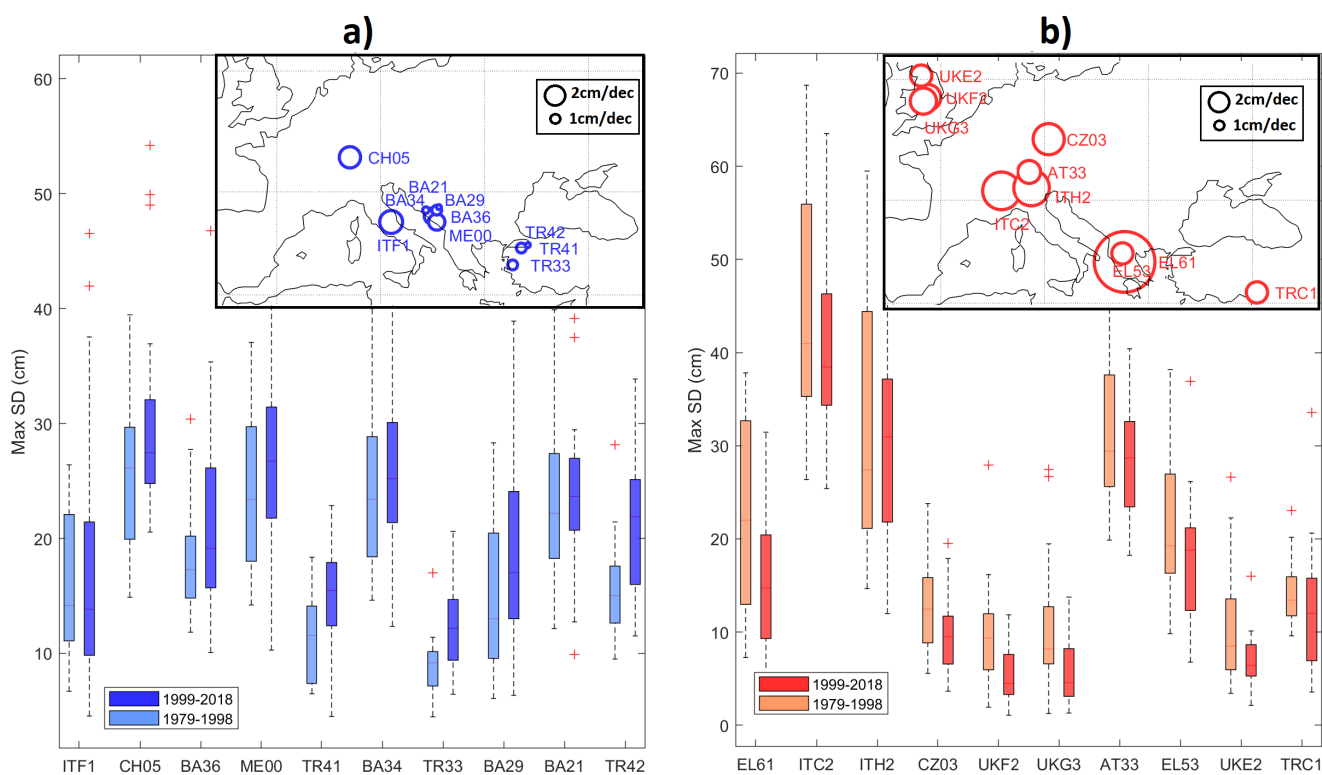


**Figure 5.** Boxplots of the maxima yearly snow-depth (SD) for two periods (1979-1998 and 1999-2018) for the 10 NUTs2 regions showing the largest negative (a) or positive (b) trends. On each box, the central mark indicates the median, and the bottom and top edges of the box indicate the 25th and 75th percentiles, respectively. The whiskers extend to the most extreme data points and the outliers are plotted individually using the '+' symbol. The insets show the location of the regions and the magnitude of trends (size of the disks).

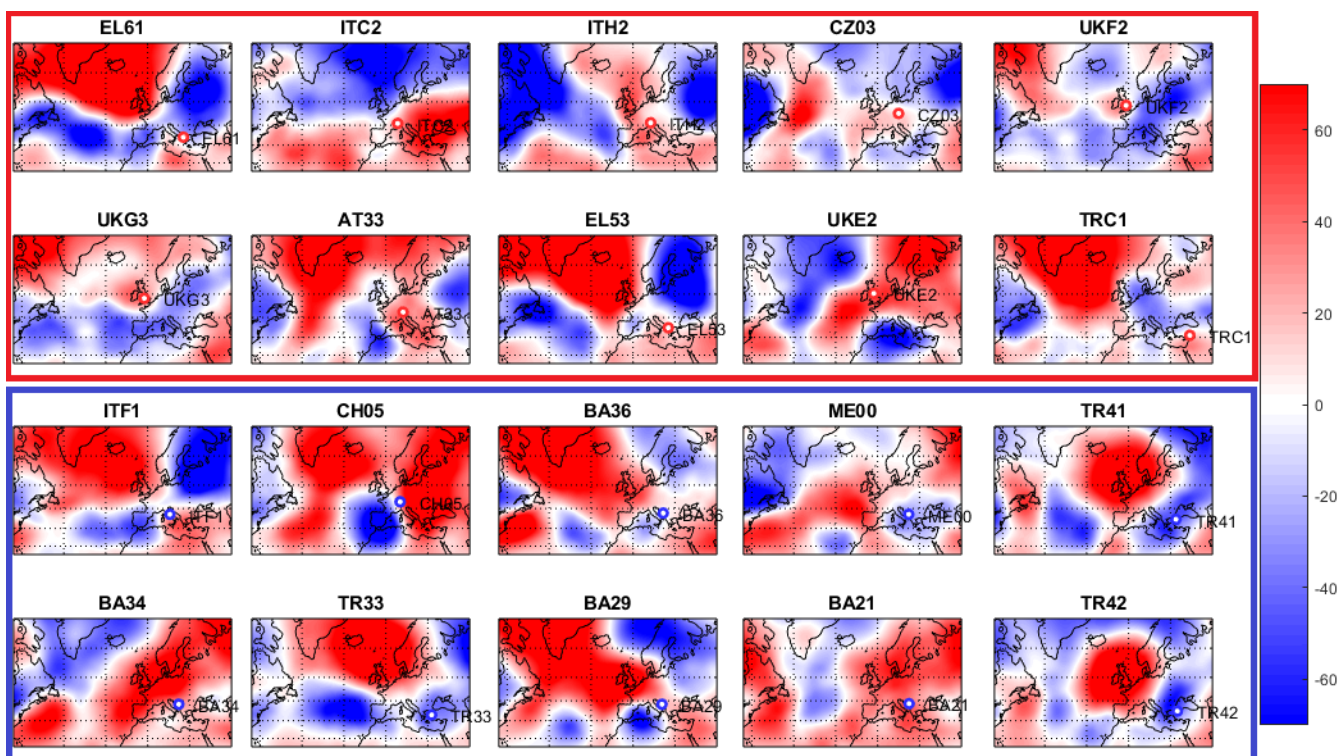


**Figure 6.** Differences between the geopotential height at 500 hPa ( $Z_{500}$ ) averaged for the 1999-2018 days of maximum snowfall and the average for the period 1979-1998, for the regions showing the largest negative (red frame) and positive (blue frame) trends.

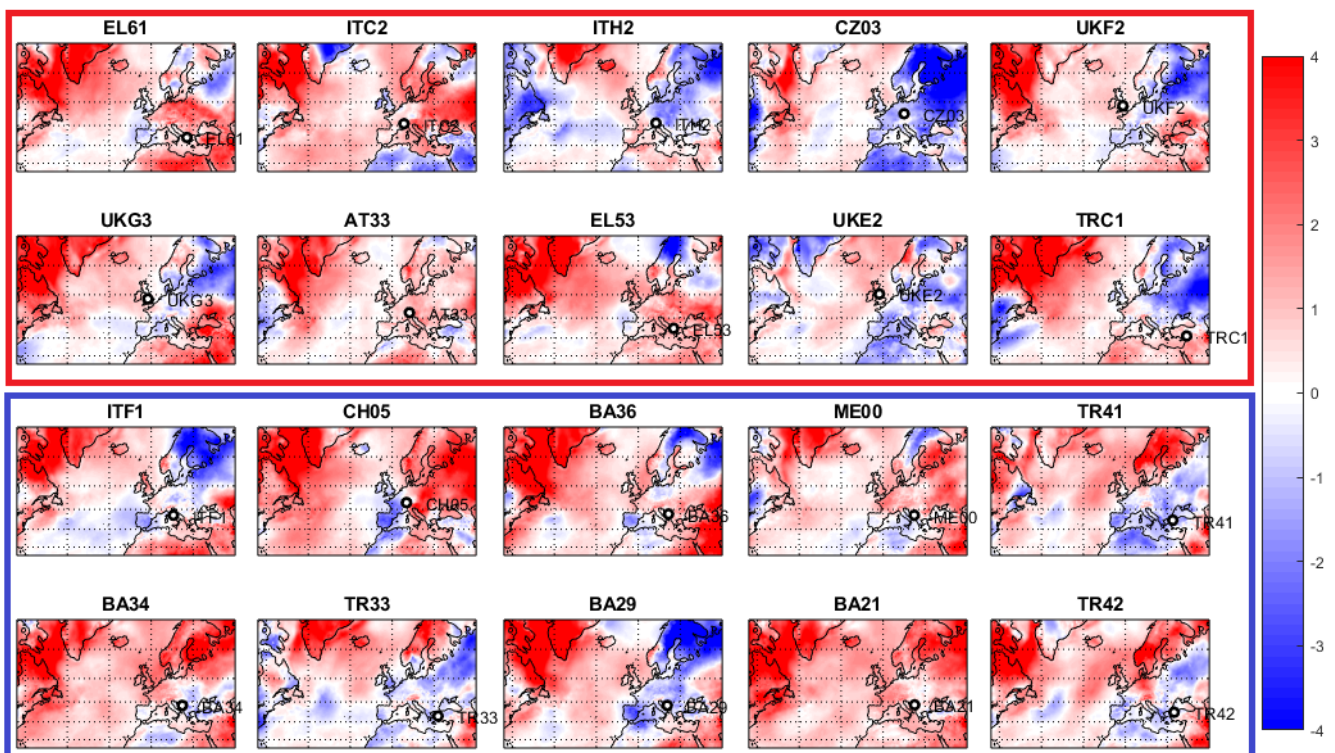


**Figure 7.** Differences between the 2m temperature averaged for the 1999-2018 days of maximum snowfall and the average for the period 1979-1998, for the regions showing the largest negative (red frame) and positive (blue frame) trends.

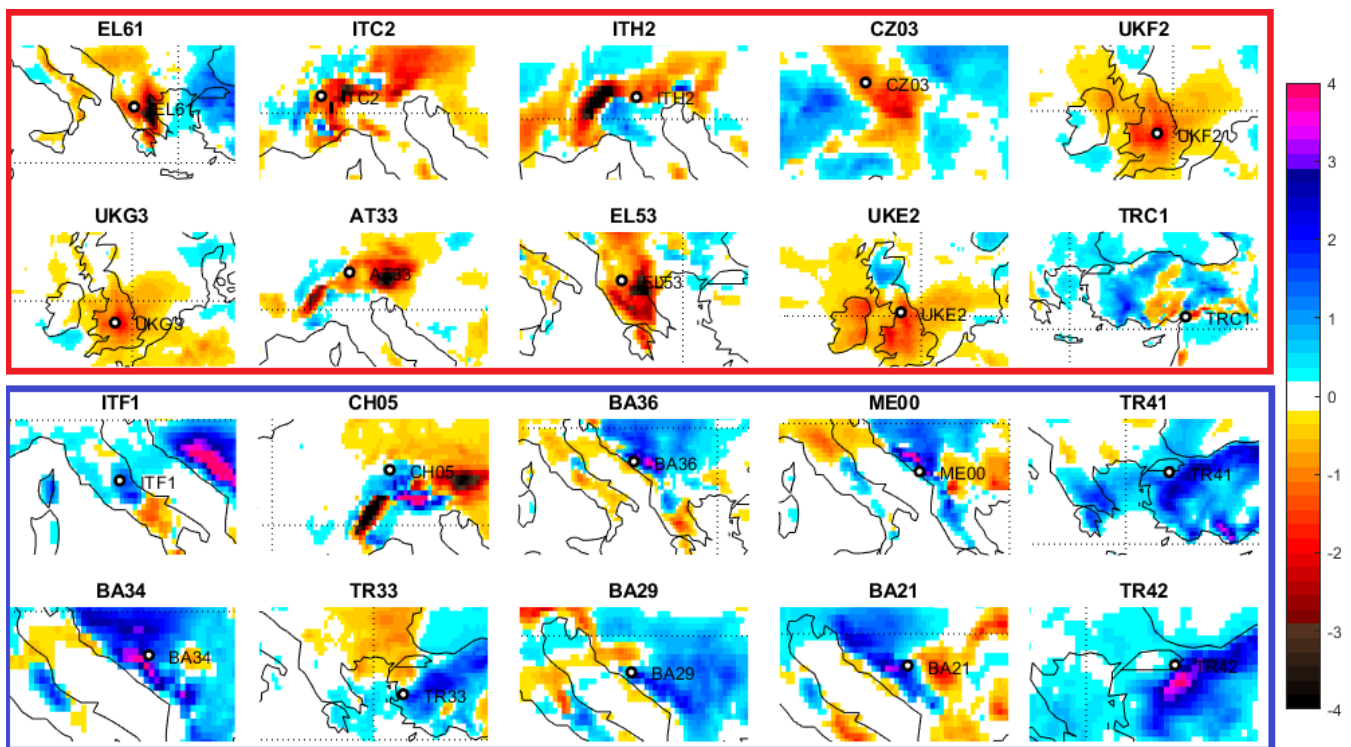


**Figure 8.** Differences between the daily snow-depth SD averaged for the 1999-2018 days of maximum snowfall and the average for the period 1979-1998, for the regions showing the largest negative (red frame) and positive (blue frame) trends.

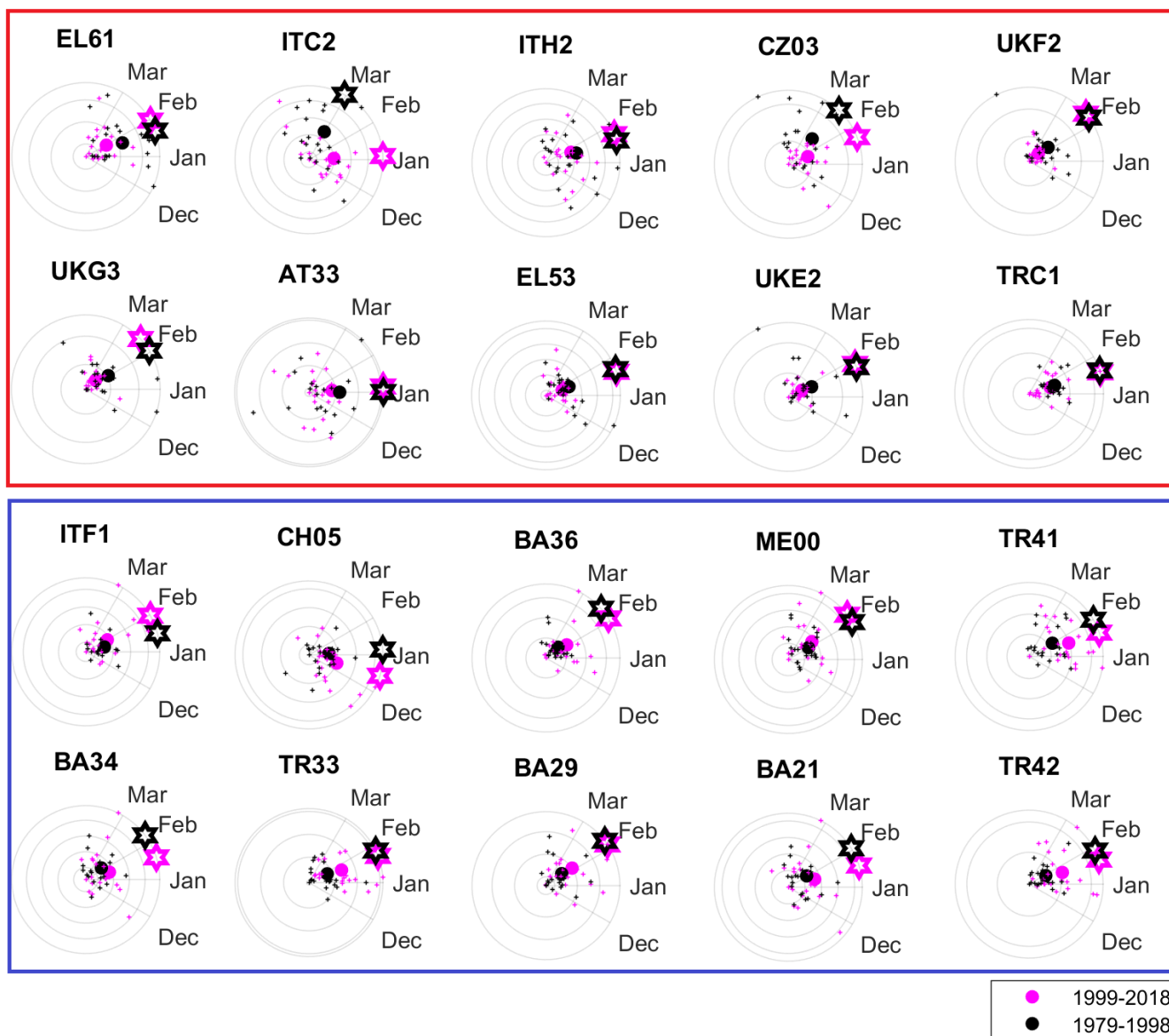


**Figure 9.** Seasonal analysis for maximum yearly snow-depth SD. The polar plots show individual maxima (small dots), averages (big dots) and average time of the year of maxima occurrence (stars) for the two different periods (1999-2018 magenta, 1979-1998 black). The angle corresponds to a date of the year in counterclockwise sense. The radius show SD magnitude relative to the largest recorded value. Only the 10 regions showing the largest negative (red frame) and positive (blue frame) trends are represented.